Top Quark Physics

SUMMARIZED FROM

HTTPS://ARXIV.ORG/PDF/1704.01356.PDF

HTTPS://ARXIV.ORG/PDF/1409.5038.PDF

HTTPS://ARXIV.ORG/PDF/1510.04483.PDF

Topics of Interest

Measurement of

- QCD production cross-section of $t\bar{t}$ pair
- Electroweak production cross-section of single top quarks
- **Mass**
- Total width (Inverse lifetime)
- CKM matrix elements involving the top quark

Tests of Standard Model (SM)

Spin correlation between pair produced top quarks

Yukawa Coupling to Higgs

Motivation and Discovery

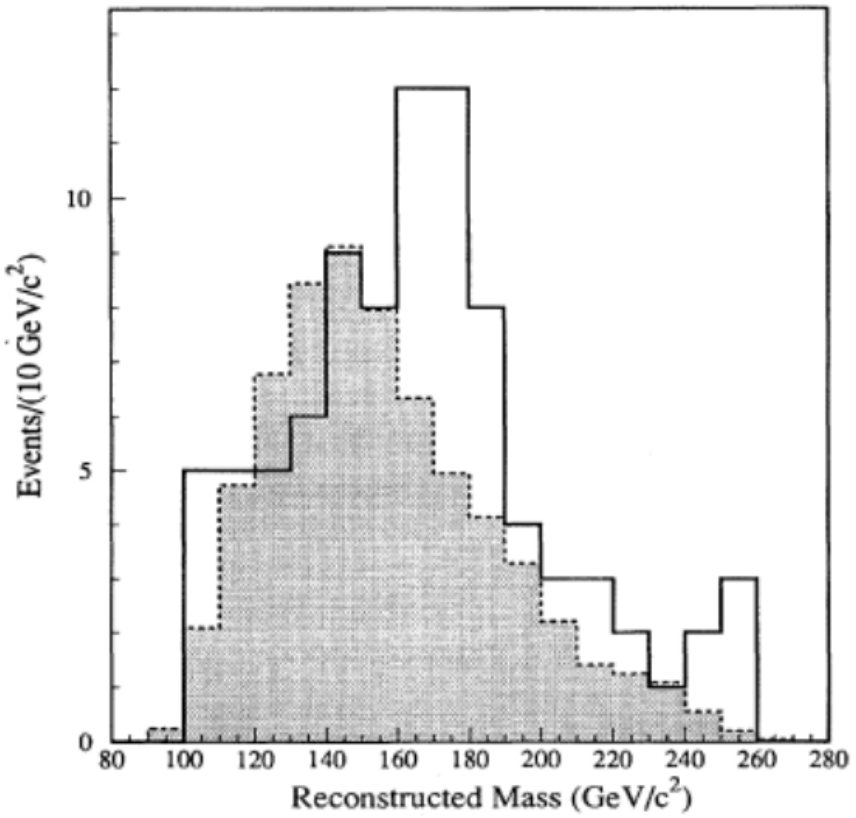

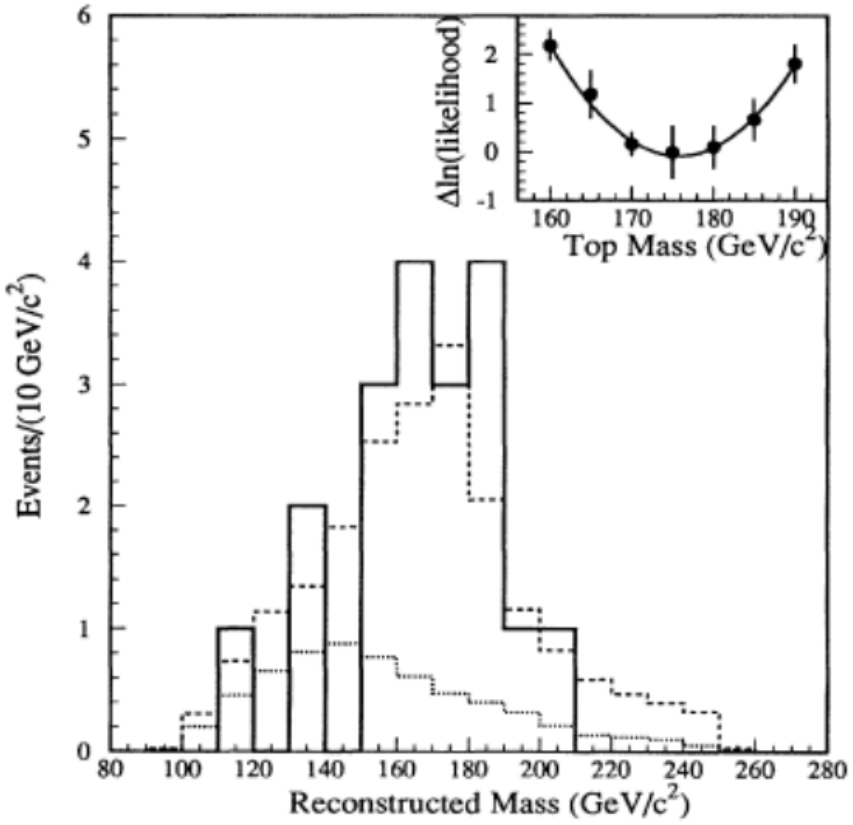

Mass distributions from CDF's top discovery paper~\cite{top-obs-1995-cdf}. Left: Reconstructed mass distribution for the $W+$ 4-jet sample prior to b tagging (solid). Also shown is the background distribution (shaded) with the normalization constrained to the calculated value. Right: Reconstructed mass distribution for the b-tagged $W+$4-jet events (solid). Also shown are the background shape (dotted) and the sum of background plus \ttbar Monte Carlo simulations for $m_t = 175$ GeV (dashed), with the background constrained to the calculated value. The inset shows the likelihood fit used to determine the top mass.

QCD $t\bar{t}$ Pair Production

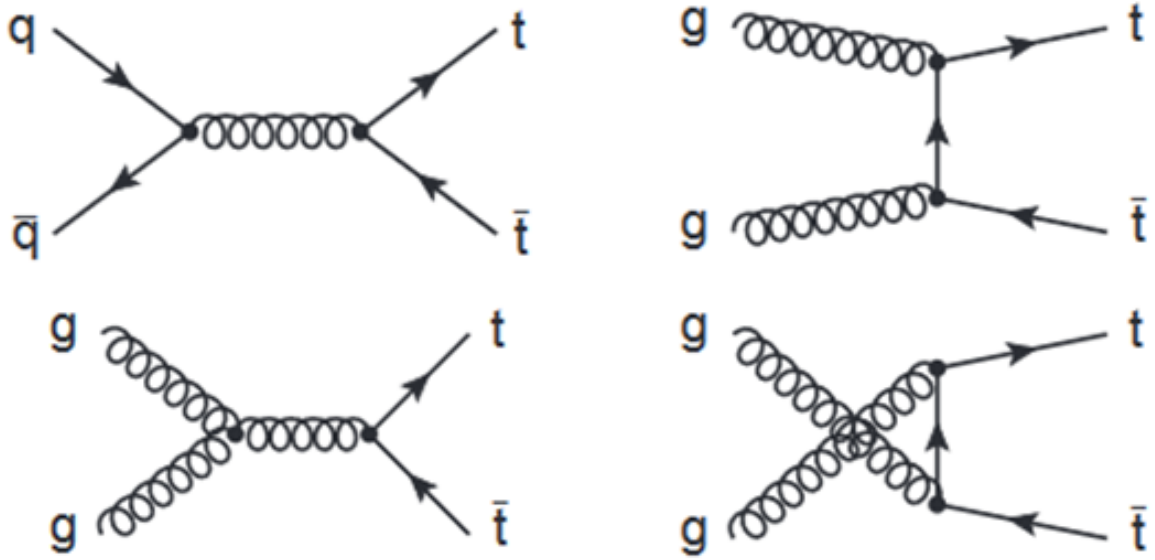

Figure 2: Feynman diagrams for $t\bar{t}$ production in QCD at LO: $q\bar{q}$ annihilation (top left), gg fusion in the s-channel (bottom left), gg fusion in the t-channel (top right), and gg fusion in the u-channel (bottom right). Feynman diagrams created with JaxoDraw [102].

Electroweak Single Top Production

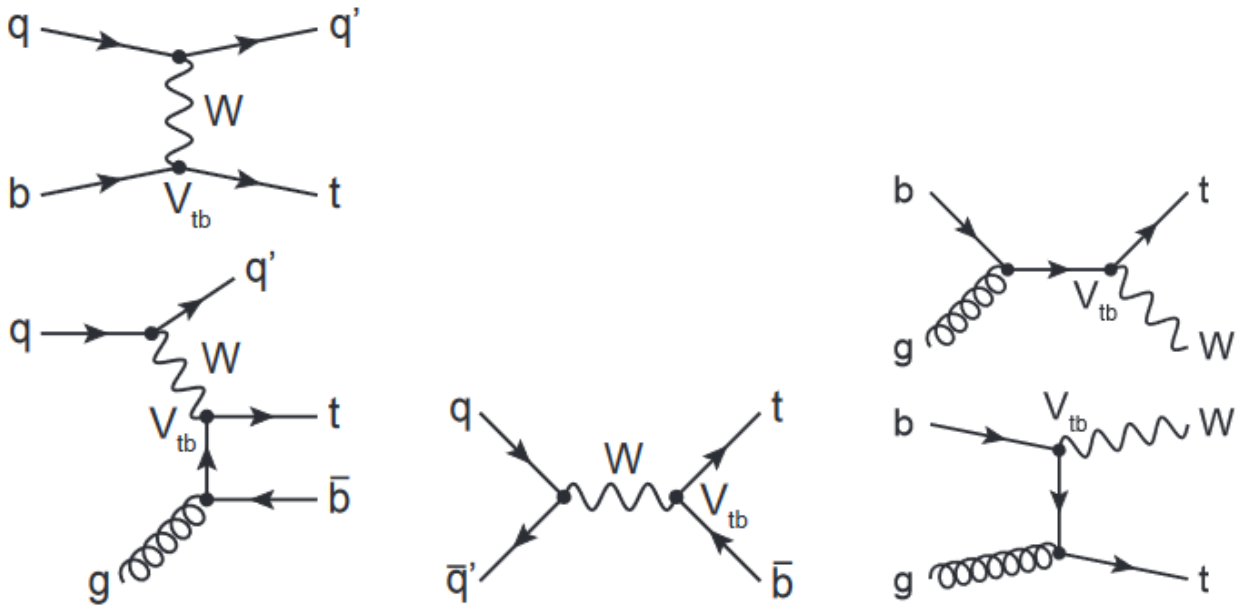

Figure 3: Feynman diagrams for electroweak single top-quark production at LO: t-channel production in the five-flavor scheme and four-flavor scheme (left), s-channel production (center), and associated Wt production (right). Feynman diagrams created with JaxoDraw [102].

Top Quark Production

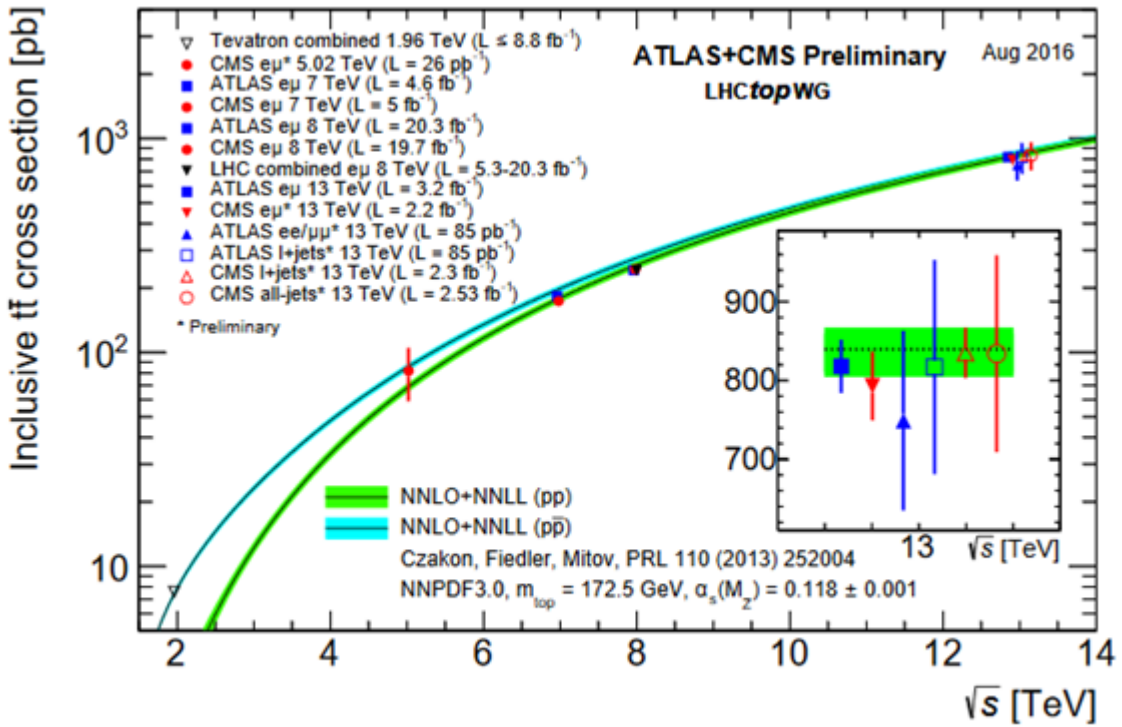

Figure 5: Compilation of measurements and SM predictions of the inclusive $t\bar{t}$ cross section as a function of the center-of-mass energy for $p\bar{p}$ collisions at the Tevatron and pp collisions at the LHC [149].

Standard Model Decay

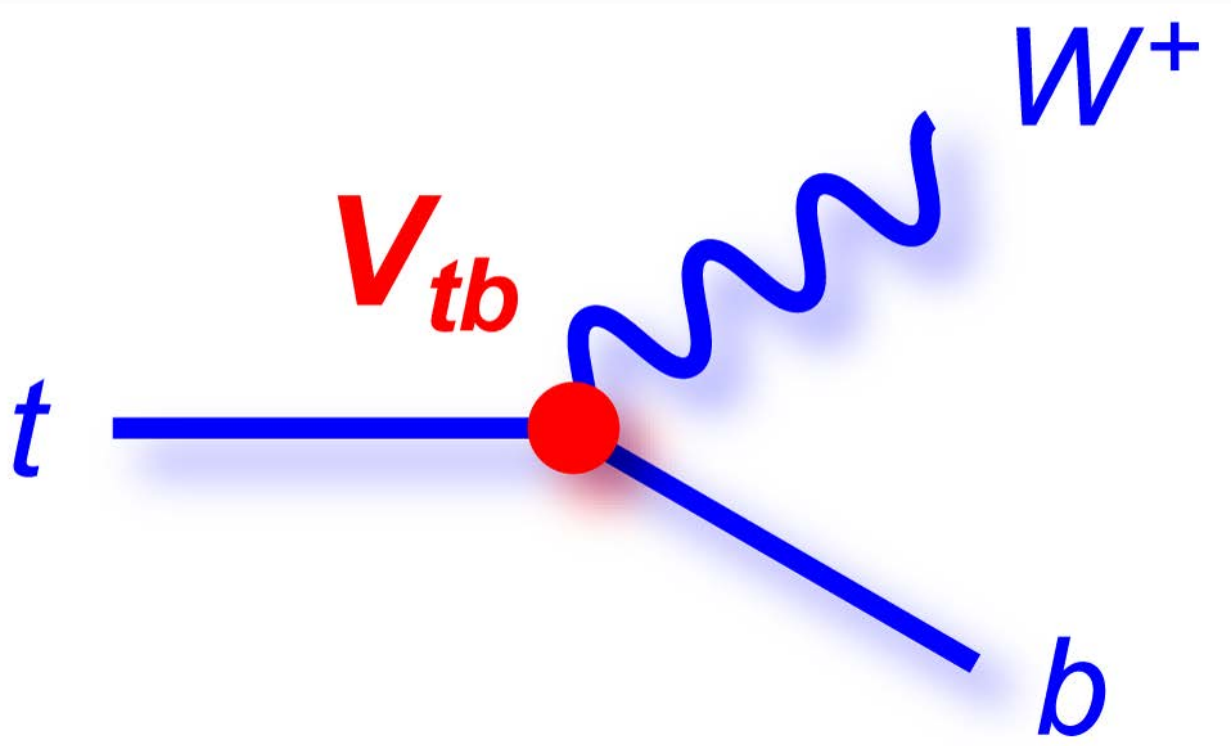

Classification of $t\bar{t}$ Decays

Fully Hadronic (branching fraction 4/9)

$t\bar{t} \rightarrow W^+ \, b \, W^- \, \bar{b} \rightarrow q \, \bar{q}' b \, q'' \, \bar{q}''' \, \bar{b}$

Semileptonic (branching fraction 2/9)

$t\bar{t} \rightarrow W^+ \, b \, W^- \, \bar{b} \rightarrow l^+ \, \nu_l \, b \, q \, \bar{q}' \, \bar{b}$

Dileptonic (branching fraction 4/81)

$t\bar{t} \rightarrow W^+ \, b \, W^- \, \bar{b} \rightarrow l^+ \, \nu_l \, b \, l'^- \, \nu_{l'} \, \bar{b}$

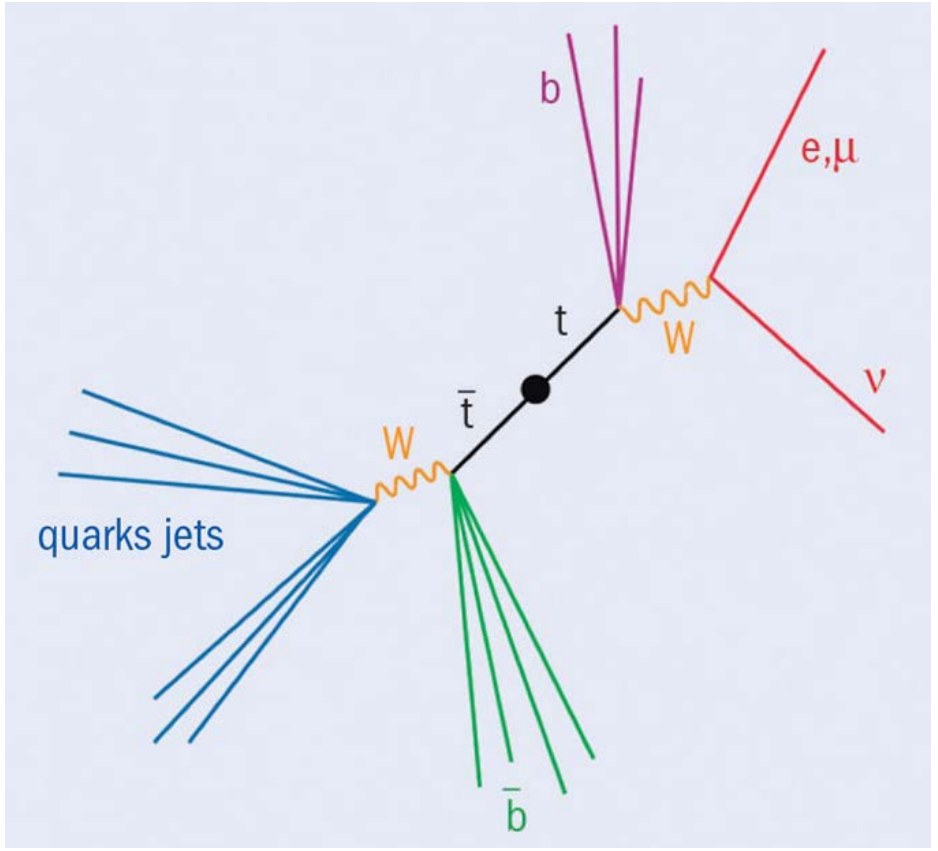

Detector Identification of Decay Products

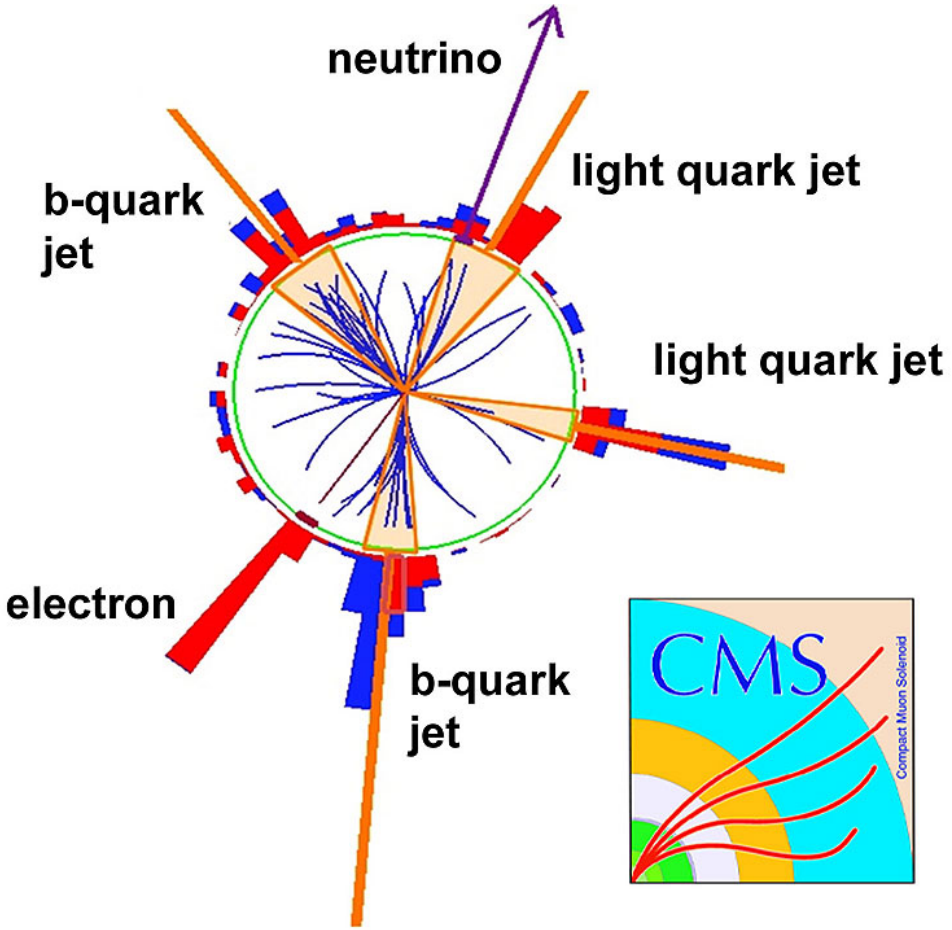

Top Quark Mass

Experiment	m_t (GeV)	stat (GeV)	syst (GeV)	total (%)
CDF	172.85	0.71	0.85	0.65
D0	174.98	0.58	0.49	0.43
ATLAS	172.99	0.41	0.74	0.49
CMS	172.35	0.16	0.48	0.29

Table 2: Summary of the most precise individual measurements of the top-quark mass m_t from the Tevatron and the LHC experiments as of November 2016, together with their statistical and systematic uncertainties as well as their total relative uncertainties.

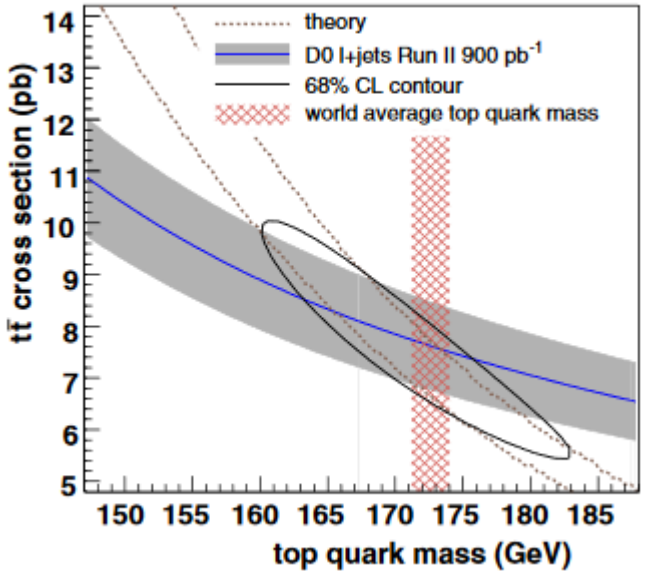

Figure 12: First determination of the top-quark mass from the $t\bar{t}$ production cross section. The cross section is obtained from the intersection of the measured and the theoretical $t\bar{t}$ cross section as a function of m_t [294].

Beyond